

Vacuum Oscillations and Future Solar Neutrino Experiments

Naoya Hata

Department of Physics, University of Pennsylvania

Philadelphia, Pennsylvania 19104-6396

(February 17, 1994, UPR-0605T)

Abstract

Vacuum oscillations are considered for the combined solar neutrino observations, including the Kamiokande II spectrum data and incorporating theoretical uncertainties and their correlations. Despite the conceptual difficulty of the fine tuning between the neutrino parameters and the Sun-Earth distance, 2-flavor vacuum oscillations provide phenomenologically acceptable solutions. There are allowed regions at 99% C.L. for $\Delta m^2 = (0.45 - 1.2) \times 10^{-10}$ eV² and $\sin^2 2\theta = 0.6 - 1$; the best fit solution is $\chi^2/\text{d.f.} = 19.2/16$, which is acceptable at 16% C.L. Oscillations for sterile neutrinos are, however, excluded by the averaged data at 99.4% C.L. The vacuum oscillation solutions predict characteristic energy spectrum distortions and seasonal variations in Sudbury Neutrino Observatory, Super-Kamiokande, and BOREXINO. Those predictions are given in detail, emphasizing that the vacuum solutions are distinguishable from the MSW solutions.

Typeset using REVTeX

I. INTRODUCTION

The solar neutrino experiments of Homestake [1,2], Kamiokande [3,4], and the gallium experiments of SAGE [5] and GALLEX [6] show significant deficits of the solar neutrino flux when compared to the standard solar model predictions [7,8], as summarized in Table I. Among many theoretical propositions to resolve the discrepancy, the astrophysical solutions in general are strongly disfavored by the observations [9–13]. Assuming the standard properties of neutrinos, the SSMs are excluded [9]. Moreover a model independent analysis concluded that the lower observed Homestake rate relative to the Kamiokande rate is essentially incompatible with all astrophysical solutions [13]. On the other hand, the neutrino oscillation hypothesis — the simplest particle physics solution requiring the minimal extension of the standard model of particle physics — fits all observations; the Mikheyev-Smirnov-Wolfenstein (MSW) [14] solutions with $\Delta m^2 \sim 10^{-5}$ eV² gives a perfect description of the data, and the obtained mass range is consistent with the general expectation of the grand unified theories with the seesaw mechanism (for recent MSW analyses, see Ref. [15] and references therein). Vacuum oscillations [16] also offer phenomenologically acceptable solutions. These, however, require a fine tuning between the neutrino parameters and the Sun-Earth distance and suffer a conceptual drawback.

In this paper the combined solar neutrino observations including the Kamiokande II spectrum data are investigated for vacuum oscillations (for other recent analysis, see Ref. [17–22]).¹ Up-to-date experimental data are used. The theoretical uncertainties and their correlations are fully incorporated. It is stressed that, since some of the flux uncertain-

¹ Vacuum oscillations were examined recently by Krastev and Petcov for the averaged data of the experiments including the theoretical uncertainties, and for the time-divided data without the theoretical uncertainties [21]. Here vacuum oscillations are studied without the time-divided data, but including the Kamiokande II spectrum data and incorporating the theoretical uncertainties, and the consequences for the future experiments are discussed.

ties are comparable to the experimental uncertainties, and also they are strongly correlated experiment to experiment and flux to flux, a careful treatment of the theoretical uncertainties is necessary. The omission of the theoretical uncertainties and their correlations can lead to a nontrivial change of the allowed parameter space [15]. From the parameter space obtained from the existing experiments, one can give robust predictions for the next generation experiments of Sudbury Neutrino Observatory, Super-Kamiokande, BOREXINO, and ICARUS, which will start operating in the mid and late 1990's. In particular the global solutions predict characteristic spectrum distortions in SNO and Super-Kamiokande and drastic seasonal variations in BOREXINO. Those predictions are explicitly given, and it is emphasized that those measurements distinguish the vacuum oscillation solutions from the MSW solutions.

II. GLOBAL ANALYSIS FOR VACUUM OSCILLATIONS

In 2-state oscillations in vacuum, the survival probability of the electron neutrinos produced in the Sun and measured in a detector is given by

$$P_{\nu_e \rightarrow \nu_e}(E, r, R) = 1 - \sin^2 2\theta \sin^2[(R - r)\Delta m^2/4E], \quad (1)$$

where Δm^2 and θ are the squared mass difference and the mixing angle between electron neutrinos and the other species of neutrinos to which ν_e 's oscillate; E is the neutrino energy and r and R are the neutrino production location and the detector location measured from the center of the Sun. As the reference SSM, the latest model including the helium diffusion effect by Bahcall and Pinsonneault is used [7]. In constraining the parameter space from the observations, the survival probability $P_{\nu_e \rightarrow \nu_e}(E, r, R)$ is convoluted with the neutrino production profile functions [7] and integrated over r , and is also averaged over the Sun-Earth distance R when compared to the time-averaged rate of the experiments. For the continuous spectrum flux components the survival probability is also integrated over E . For the radiochemical detectors the detector cross sections are taken from Ref. [23,24] and

included; for Kamiokande the detector cross section, the detector resolution, and the detector efficiency are included [3]. When the Kamiokande II spectrum data are incorporated, the electron spectrum are divided into 14 bins according to the published data [3].

Since the theoretical uncertainty of the ${}^8\text{B}$ flux (14%) in the Bahcall-Pinsonneault SSM is comparable to the experimental uncertainties of Homestake (11%) and Kamiokande (14%), it is important to incorporate the theoretical uncertainties of the neutrino fluxes in the analysis. The flux uncertainties are strongly correlated experiment to experiment, and also flux to flux. The SSM uncertainties are parametrized with the uncertainties of the central temperature and the uncertainties of the relevant nuclear reaction cross sections, following the prescription described in Ref. [15]. The uncertainties from the detector cross sections are also included and are correlated between the two gallium experiments.

First the analysis has been carried out for Homestake, SAGE, GALLEX, and the averaged rate of Kamiokande II and III without the spectrum data. The two gallium experiments are treated as independent data points. When we confront observations to a theory, there are two statistical questions to ask:

1. Given the observations, is the theory acceptable or not?
2. Once we decide that the theory is acceptable, what is the allowed parameter space in the theory at a certain confidence level?

In the present case, the first question is quantified by evaluating the goodness-of-fit (GOF) for the χ^2 minimum in the $\Delta m^2 - \sin^2 2\theta$ space. The global χ^2 minimum when the data are fit to the oscillation parameters is 5.0 for 2 degrees of freedom (2 d.f. = 4 experiments – 2 parameters). The probability of obtaining the χ^2 minimum equal to or larger than 5.0 for 2 d.f. by chance is 8%. That is, the best fit solution for vacuum oscillations is allowed at the 8% confidence level (C.L.), which is not an excellent fit, but acceptable. There are seven local χ^2 minima in the region $\Delta m^2 = (0.35 - 1.3) \times 10^{-10} \text{ eV}^2$ and $\sin^2 2\theta = 0.6 - 1.0$; their oscillation parameters, χ^2 , and the GOF values are summarized in Table II.

The data have also been fit to Δm^2 , $\sin^2 2\theta$, and the mean Sun-Earth distance simultaneously. For the best fit solution (Solution D in Table II), the mean Sun-Earth distance has to be fine-tuned within 5% to describe the existing observations at 90% C.L. Unless we invoke some kind of anthropic principle, there is no apparent logical connections between the oscillation parameters and the Sun-Earth distance, and this fine tuning is considered as a conceptual drawback in vacuum oscillations.

Once vacuum oscillations are accepted as a phenomenologically viable theory for the solar neutrino observations, the C.L. regions are obtained by evaluating χ^2 at each point in the $\Delta m^2 - \sin^2 2\theta$ space. The allowed regions are defined by

$$\chi^2(\sin^2 2\theta, \Delta m^2) \leq \chi_{\min} + \Delta\chi^2, \quad (2)$$

where χ_{\min} is the global χ^2 minimum, and $\Delta\chi^2 = 4.6$, 6.0, and 9.2 for 90, 95, and 99% C.L., respectively.² The constraints obtained from each Homestake, Kamiokande, and the combined gallium experiment at 95% C.L. are shown in Fig. 1.

When the parameters are fit with the combined observations, the allowed regions are essentially controlled by the Homestake data and limited to $\Delta m^2 = (0.35 - 1.3) \times 10^{-10} \text{ eV}^2$ and $\sin^2 2\theta = 0.6 - 1.0$. The regions allowed by the combined observations at 90, 95, and 99% C.L. are shown in Fig. 2; the allowed regions are essentially in agreement with the recent analysis by Krastev and Petcov [21]. The slight differences are mainly due to the difference in the input data.

Since the ν_e survival probability in this parameter space (i.e., the Sun-Earth distance \sim the oscillation length) are often energy dependent, the analysis has been also carried out with the additional Kamiokande II energy spectrum data. The 14 data points obtained

²This definition of the allowed parameter space assumes a gaussian distribution of the probability density around the global χ^2 minimum. That is, the allowed regions should have elliptical shape, and this is only a crude approximation in the present case. Therefore the allowed regions shown in Fig. 1, 2, and 4 should be taken as qualitative displays of confidence levels.

in the Kamiokande II experiment are used [3]; the theoretical uncertainties as well as the experimental systematic uncertainties ($0.06 \times \text{SSM}$) are correlated among the 14 bins. No spectrum data are available from Kamiokande III and the average value is used as an independent data point. The SSM flux uncertainties are also correlated between Kamiokande II and III.³ The expected spectrum distortions for three local minima (B, D, and F) for Kamiokande along with the actual Kamiokande II data are shown in Fig. 3. The global χ^2 minimum of the combined analysis is 19.2 for 16 d.f. ($= 18$ data points – 2 parameters), which is acceptable at 84% C.L. The neutrino parameters and the GOF for all local χ^2 minima in this region are listed in Table III. The allowed parameter regions are displayed in Fig. 4. The parameter space allowed at 99% C.L. is for

$$\Delta m^2 = (0.45 - 1.2) \times 10^{-10} \text{ eV}^2 \text{ and } \sin^2 2\theta = 0.6 - 1.0, \quad (3)$$

and remain essentially unchanged by including the Kamiokande II spectrum information.

Vacuum oscillations can also be considered between electron neutrinos and sterile neutrinos [25,17,19,21]. In this case there are no neutral current events from the transformed neutrinos in Kamiokande, which would be present and contribute about 15% of the total signal in the case of oscillations into ν_μ or ν_τ . This absence of the neutral current contributions in Kamiokande makes the difference between the Kamiokande rate and the Homestake rate effectively wider, and the fits become considerably worse. In the joint χ^2 analysis without the Kamiokande spectrum data, the global χ^2 minimum is 10.1 for 2 d.f., which is an extremely poor fit. The GOF is 0.63%, and the solution is excluded at 99.4% C.L. That is, including all theoretical and experimental uncertainties, the existing experiments are essentially incompatible with vacuum oscillation for sterile neutrinos.⁴ When the Kamiokande II

³ The possible correlations of the systematic uncertainties in Kamiokande II and Kamiokande III were ignored.

⁴ The same conclusion was obtained by Krastev and Petcov [21], but with less statistical significance. The difference is entirely due to the difference in the input data.

spectrum data are included, the GOF improves (4.8%), but this is an artifact of increasing the number of degrees of freedom by adding the Kamiokande II 14 bins, and does not mean that the sterile oscillations are favored by the Kamiokande spectrum data; the incompatibility of the data and the sterile oscillations remains essentially unchanged. The oscillation parameters and GOF for each χ^2 local minimum is listed in Table IV for the averaged rate, and in Table V for the analysis including the Kamiokande II spectrum data.

III. PREDICTIONS FOR THE FUTURE SOLAR NEUTRINO EXPERIMENTS

The oscillation hypothesis for the solar neutrinos, either the MSW mechanism or the vacuum oscillations, will be verifiable in the next-generation solar neutrino experiments of SNO [26], Super-Kamiokande [27], BOREXINO [28], and ICARUS [29]. Moreover those experiments should be able to distinguish the vacuum solutions and the MSW solutions, and determine the oscillation parameters accurately. The key measurements in those experiments are:

1. The ratio of charged and neutral current events (CC/NC) from the ${}^8\text{B}$ neutrinos in SNO.
2. The energy spectrum measurements in SNO and Super-Kamiokande.
3. The measurements of time variations of the ${}^8\text{B}$ neutrinos in SNO and Super-Kamiokande, and the measurements of time variations of the ${}^7\text{Be}$ neutrinos in BOREX-INO.

The CC/NC measurement in SNO is the gold plated observable in confirming or falsifying the oscillation hypothesis. The comparison of the observed value $(\text{CC/NC})_{\text{SNO}}$ and the SSM value $(\text{CC/NC})_{\text{SSM}}$ is free from the SSM flux uncertainties, and a depletion of the observed charged current signifies the oscillations between ν_e and ν_μ or ν_τ . Assuming the Bahcall-Pinsonneault SSM, the currently allowed parameter space at 95% C.L. predicts

$$\frac{(CC/NC)_{SNO}}{(CC/NC)_{SSM}} = 0.15 - 0.5. \quad (4)$$

There are two caveats, however. The CC/NC measurement by itself does not distinguish the type of oscillations (e.g., whether the MSW effect or vacuum oscillations). Also $(CC/NC)_{SNO}$ is the same as $(CC/NC)_{SSM}$ if the oscillations are for sterile neutrinos. The measurements of the energy spectrum and of time variations are important in determining those detailed features of neutrino oscillations. In the following, the predictions for spectrum distortions and the time variations are discussed separately, but those two effects are often strongly correlated, and the real data in the future experiments should be analyzed accordingly.

Although the existing Kamiokande energy spectrum data do not significantly constrain the parameter space, the next generation experiments with high statistics and with lower energy thresholds (~ 5 MeV) are quite sensitive to the spectrum distortions caused by oscillations. In Fig. 5, the expected spectrum shapes are displayed for three vacuum solutions (B, D, and F defined in Table III) along with the spectra expected from the MSW solutions obtained by the global analysis; the MSW large-angle solution has little distortion and is identical to the astrophysical solutions. The spectra are normalized above the proposed detector threshold (5 MeV). The charged current cross section [30,31] and the detector resolutions [26] are also included.⁵ The error bars correspond to the statistical uncertainties for a total of 6,000 events (equivalent to 2 year operation). The vacuum oscillations are clearly distinguishable from the MSW solutions and the astrophysical solutions. The similar predictions for Super-Kamiokande are displayed in Fig. 6 with error bars corresponding to a total of 16,000 events (2 year operation).

⁵In the SNO spectrum analysis, it is important to include the effect of the continuous spectrum of the out-going electrons and also the detector resolution: the approximation of the out-going electron spectra from the monoenergetic neutrinos with a delta function (i.e., “observed electron energy” = “neutrino energy” – 1.44 MeV) significantly overestimates the detector sensitivity for spectrum distortions and is inappropriate for the spectrum shape analysis.

The survival probability [Eqn. (1)] is also sensitive to the Sun-Earth distance R and the solutions of the combined observation predict seasonal variations of the solar neutrino signal due to the eccentricity of the Earth orbit. Especially drastic time variations are expected for the ${}^7\text{Be}$ neutrino signals since they are mono-energetic (therefore not smeared out by the energy integral), and also the oscillation length is shorter than for most of the ${}^8\text{B}$ neutrinos [17,19,21]. For the existing experiments the expected time variations for the global solutions (B, D, and F) are displayed in Fig. 7: the error bars are the statistical uncertainties when (overly optimistic) large number of events are assumed: 500, 1,000, and 1,000 events for Kamiokande, Homestake, and the gallium experiment, while the currently accumulated signals are ~ 200 , ~ 500 , and ~ 50 events, respectively. Obviously there is little chance of detecting the seasonal variations by the currently operating experiments.

The time variations expected in SNO, Super-Kamiokande, and BOREXINO are shown in Fig. 8: the error bars are for the total number of events 12,000, 32,000, and 12,000, respectively (each corresponds to 4 years of operation). The seasonal variations should be observable in these experiments. In particular the time variations are most drastic in BOREXINO because of its sensitivity for the ${}^7\text{Be}$ neutrinos. Those measurements are unmistakable and should provide strong constraints on the oscillation parameters.

IV. CONCLUSION

The Homestake, SAGE, GALLEX and Kamiokande data including the Kamiokande II spectrum data are analyzed for neutrino oscillations in vacuum. There are phenomenologically acceptable solutions in $\Delta m^2 = (0.45-1.2) \times 10^{-10} \text{ eV}^2$ and $\sin^2 2\theta = 0.6-1.0$, although these solutions suffer from the fine tuning between the oscillation parameters and the Sun-Earth orbit. Oscillations for sterile neutrinos are strongly disfavored by the observations and are excluded at 99.4% C.L. The acceptable solutions for the flavor oscillations predict characteristic energy spectrum distortions and seasonal variations in the next generation solar neutrino experiments. The measurements of these signals should distinguish the vacuum

oscillations from the astrophysical solutions as well as from the MSW solutions.

ACKNOWLEDGMENTS

I thank Paul Langacker for his encouragement, useful comments, and careful reading of the manuscript. It is also a pleasure to thank Eugene Beier and Sidney Bludman for useful discussions. I thank Plamen Krastev for directing my attention to the importance of measuring the time variations of the ${}^7\text{Be}$ flux. This work was supported by the Department of Energy Contract No. DE-AC02-76-ERO-3071.

REFERENCES

- [1] R. Davis Jr. *et al.*, in *Proceedings of the 21th International Cosmic Ray Conference*, Vol. 12, edited by R. J. Protheroe (University of Adelaide Press, Adelaide, 1990), p. 143; R. Davis Jr., in *Frontiers of Neutrino Astrophysics*, edited by Y. Suzuki and K. Nakamura (Universal Academy Press, Tokyo, 1993) p. 47.
- [2] K. Lande, private communications; B. Cleveland, private communications.
- [3] Kamiokande II Collaboration, K. S. Hirata *et al.*, Phys. Rev. Lett. **65**, 1297 (1990); **65**, 1301(1990); **66**, 9 (1991); Phys. Rev. D **44**, 2241 (1991).
- [4] A. Suzuki, KEK report No. 93-96, 1993 (unpublished). Y. Suzuki, in *Frontiers of Neutrino Astrophysics*, edited by Y. Suzuki and K. Nakamura (Universal Academy Press, Tokyo, 1993) p. 61.
- [5] SAGE Collaboration, A. I. Abazov, *et al.*, Phys. Rev. Lett. **67**, 3332 (1991); V. N. Gavrin, in *TAUP*, Gran Sasso, Italy, September, 1993.
- [6] GALLEX Collaboration, P. Anselmann *et al.*, Phys. Lett. B **285**, 376 (1992); **285**, 390 (1992); **314**, 445 (1993).
- [7] J. N. Bahcall and M. H. Pinsonneault, Rev. Mod. Phys. **64**, 885 (1992).
- [8] S. Turck-Chièze and I. Lopes, Astrophys. J. **408**, 347 (1993). S. Turck-Chièze, S. Cahen, M. Cassé, and C. Doom, Astrophys. J. **335**, 415 (1988).
- [9] J. N. Bahcall and H. A. Bethe, Phys. Rev. D **47**, 1298 (1993); Phys. Rev. Lett. **65**, 2233 (1990); H. A. Bethe and J. N. Bahcall, Phys. Rev. D **44**, 2962 (1991).
- [10] S. Bludman, D. Kennedy, and P. Langacker, Phys. Rev. D **45**, 1810 (1992); Nucl. Phys. B **374**, 373 (1992).
- [11] S. Bludman, N. Hata, D. Kennedy, and P. Langacker, Phys. Rev. D **47**, 2220 (1993).
- [12] V. Castellani, S. Degl'Innocenti, and G. Fiorentini, Astron. Astrophys. **271**, 601 (1993).

[13] N. Hata, S. Bludman, and P. Langacker, University of Pennsylvania preprint, UPR-0572T, 1993 (to be published in Phys. Rev. D).

[14] L. Wolfenstein, Phys. Rev. D **17**, 2369 (1978); **20**, 2634 (1979); S. P. Mikheyev and A. Yu. Smirnov, Yad. Fiz. **42**, 1441 (1985) [Sov. J. Nucl. Phys. **42** 913 (1985)]; Nuovo Cimento **9C**, 17 (1986).

[15] N. Hata and P. Langacker, University of Pennsylvania Preprint No. UPR-0592T, 1993 (submitted to Phys. Rev. D).

[16] B. Pontecorvo, Zh. Eksp. Teor. Fiz. **33**, 549 (1957); **34**, 247 (1958); **53**, 1717 (1967); S. M. Bilenky and B. Pontecorvo, Phys. Rep. **41**, 225 (1978); S. L. Glashow and L. M. Krauss, Phys. Lett. B **190**, 199 (1988).

[17] V. Barger, R. J. N. Phillips, and K. Whisnant, Phys. Rev. D **43**, 1110 (1991); Phys. Ref. Lett. **69**, 3135 (1992).

[18] A. Acker, S. Pakvasa, and J. Pantaleone, Phys. Rev. D **43**, 1754 (1991).

[19] P. I. Krastev and S. T. Petcov, Phys. Lett. B **285**, 85 (1992); Phys. Lett. B **299**, 99 (1993).

[20] A. Acker, A. B. Balantekin, and F. Loret, University of Wisconsin at Madison Preprint No. MAD-NT-93-06, 1993 (unpublished).

[21] P. I. Krastev and S. T. Petcov, Preprint No. IFP-480-UNC, SISSA 177/93/EP, 1993 (unpublished).

[22] R. J. N. Phillips, Rutherford Appleton Laboratory Report No. RAL-94-017, 1994 (unpublished).

[23] J. N. Bahcall and R. N. Ulrich, Rev. Mod. Phys. **60**, 297 (1988).

[24] J. N. Bahcall, *Neutrino Astrophysics*, (Cambridge University Press, Cambridge, England, 1989).

[25] P. Langacker, University of Pennsylvania Report No., UPR 0401T (1989); R. Barbieri and A. Dolgov, Nucl. Phys. B **349**, 743 (1991); K. Enqvist, K. Kainulainen, and J. Maalampi, Phys. Lett. B **249**, 531 (1990); M. J. Thomson and B. H. J. McKellar, Phys. Lett. B **259**, 113 (1991); V. Barger *et al.*, Phys. Rev. D **43**, 1759 (1991); P. Langacker and J. Liu, Phys. Rev. D **46**, 4140 (1992).

[26] G. T. Ewan *et al.* “Sudbury Neutrino Observatory Proposal”, Report No. SNO-87-12, 1987 (unpublished); “Scientific and Technical Description of the Mark II SNO Detector”, edited by E. W. Beier and D. Sinclair, Report No. SNO-89-15, 1989 (unpublished).

[27] Y. Totsuka, University of Tokyo (ICRR) Report No. ICCR-Report-227-90-20, 1990 (unpublished).

[28] “BOREXINO at Gran Sasso — proposal for a real time detector for low energy solar neutrinos”, Vol. 1, edited by G. Bellini, M. Campanella, D. Giugni, and R. Raghavan, 1991, (unpublished).

[29] C. Rubbia, Report CERN No. CERN-PPE/93-08, 1993 (unpublished).

[30] S. Nozawa, private communications.

[31] M. Doi and K. Kubodera, Phys. Rev. C **45**, 1988 (1992); S. Ying, W. Haxton, and E. Henley Phys. Rev. C **45**, 1982 (1992); K. Kubodera and S. Nozawa, University of South Carolina Report No. USC(NT)-93-6 (unpublished) and references therein.

TABLES

TABLE I. The standard solar model predictions of Bahcall and Pinsonneault [7] (BP SSM) and of Turck-Chièze and Lopes [8] (TCL SSM). The Bahcall-Pinsonneault model includes the helium diffusion effect, while the Turck-Chièze-Lopes model does not. Also shown are the results of the solar neutrino experiments. The gallium experiment is the combined result of SAGE and GALLEX I and II.

	BP SSM	TCL SSM	Experiments
Kamiokande ^a	1 ± 0.14	0.77 ± 0.19	0.51 ± 0.07 BP SSM
Homestake ^b (SNU)	8 ± 1	6.4 ± 1.4	2.34 ± 0.26 (0.29 ± 0.03 BP SSM)
Ga experiment (SNU)	131.5 ± 7	122.5 ± 7	81 ± 13 (0.62 ± 0.10 BP SSM)
SAGE ^c (SNU)			70 ± 22 (0.53 ± 0.16 BP SSM)
GALLEX ^d (SNU)			87 ± 16 (0.66 ± 0.12 BP SSM)

^aThe result of the combined data of 1040 days of Kamiokande II [0.47 ± 0.05 (stat) ± 0.06 (sys) BP SSM] [3] and 514.5 days of Kamiokande III [0.57 ± 0.06 (stat) ± 0.06 (sys) BP SSM] [4].

^bThe result of Run 18 to 122 is 2.34 ± 0.16 (stat) ± 0.21 (sys) SNU [2].

^cThe preliminary result of SAGE I (from January, 1990 through May, 1992) is 70 ± 19 (stat) ± 10 (sys) SNU [5].

^dThe combined result of GALLEX I and II (including 21 runs through April, 1993) is 87 ± 14 (stat) ± 7 (sys) SNU [6].

TABLE II. The solutions for vacuum oscillations when the combined result of Homestake, Kamiokande, SAGE, and GALLEX is used. The SAGE and GALLEX data are fit separately. The Kamiokande II spectrum data are not included. A – G correspond to seven local χ^2 minima within the allowed regions at 99% C.L. The goodness-of-fit (GOF) is the probability of obtaining by chance a χ^2 minimum value equal to or larger than the value we actually obtained.

	Δm^2 (eV 2)	$\sin^2 2\theta$	χ^2 (2 d.f.)	GOF (%)
A	1.2×10^{-10}	1.00	10.9	0.42
B	1.0×10^{-10}	0.96	5.7	5.9
C	9.0×10^{-11}	0.84	5.1	7.9
D	7.9×10^{-11}	0.78	5.0	8.0
E	6.3×10^{-11}	0.81	5.2	7.6
F	5.2×10^{-11}	0.99	7.5	2.3
G	3.8×10^{-11}	1.00	14.5	0.071

TABLE III. Same as Table II except that the Kamiokande II spectrum data are included.

	Δm^2 (eV 2)	$\sin^2 2\theta$	χ^2 (16 d.f.)	GOF (%)
A	1.2×10^{-10}	1.00	25.4	3.1
B	1.0×10^{-10}	0.91	20.5	12
C	9.1×10^{-11}	0.82	19.2	16
D	7.8×10^{-11}	0.78	19.2	16
E	6.5×10^{-11}	0.80	20.4	12
F	5.2×10^{-11}	0.99	23.7	4.9
G	3.8×10^{-11}	1.00	29.9	0.79

TABLE IV. The solutions for vacuum oscillations for sterile neutrinos when the combined result of Homestake, Kamiokande, SAGE, and GALLEX is used. The SAGE and GALLEX data are fit separately. The Kamiokande II spectrum data are not included. A – G correspond to seven local χ^2 minima within the region.

	Δm^2 (eV 2)	$\sin^2 2\theta$	χ^2 (2 d.f.)	GOF (%)
A	1.2×10^{-10}	1.00	13.5	0.12
B	1.1×10^{-10}	0.88	10.1	0.63
C	9.1×10^{-11}	0.79	11.0	0.42
D	7.8×10^{-11}	0.75	11.0	0.41
E	6.3×10^{-11}	0.78	10.4	0.56
F	5.0×10^{-11}	0.93	12.7	0.18
G	3.8×10^{-11}	1.00	16.5	0.026

TABLE V. Same as Table IV except that the Kamiokande II spectrum data are included.

	Δm^2 (eV 2)	$\sin^2 2\theta$	χ^2 (16 d.f.)	GOF (%)
A	1.2×10^{-10}	0.98	30.1	1.7
B	1.1×10^{-10}	0.84	27.0	4.2
C	9.1×10^{-11}	0.78	27.6	3.5
D	7.8×10^{-11}	0.74	27.1	4.1
E	6.3×10^{-11}	0.77	26.4	4.8
F	5.0×10^{-11}	0.91	29.3	2.2
G	3.8×10^{-11}	1.00	32.3	0.92

FIGURES

FIG. 1. The allowed parameter space at 95% C.L. for the Homestake, Kamiokande and combined gallium experiments of SAGE and GALLEX including the theoretical uncertainties and their correlations. The Kamiokande II spectrum data are not included.

FIG. 2. The parameter space allowed by the combined observation of the Homestake, Kamiokande, and the combined gallium experiments of SAGE and GALLEX, including the theoretical uncertainties and their correlations. The Kamiokande II spectrum data are not included.

FIG. 3. The spectrum shape divide by the SSM spectrum expected in Kamiokande. The shape is shown for the combined solutions B, D, and F, which are listed in Table III. Also shown are the Kamiokande II spectrum data [3]

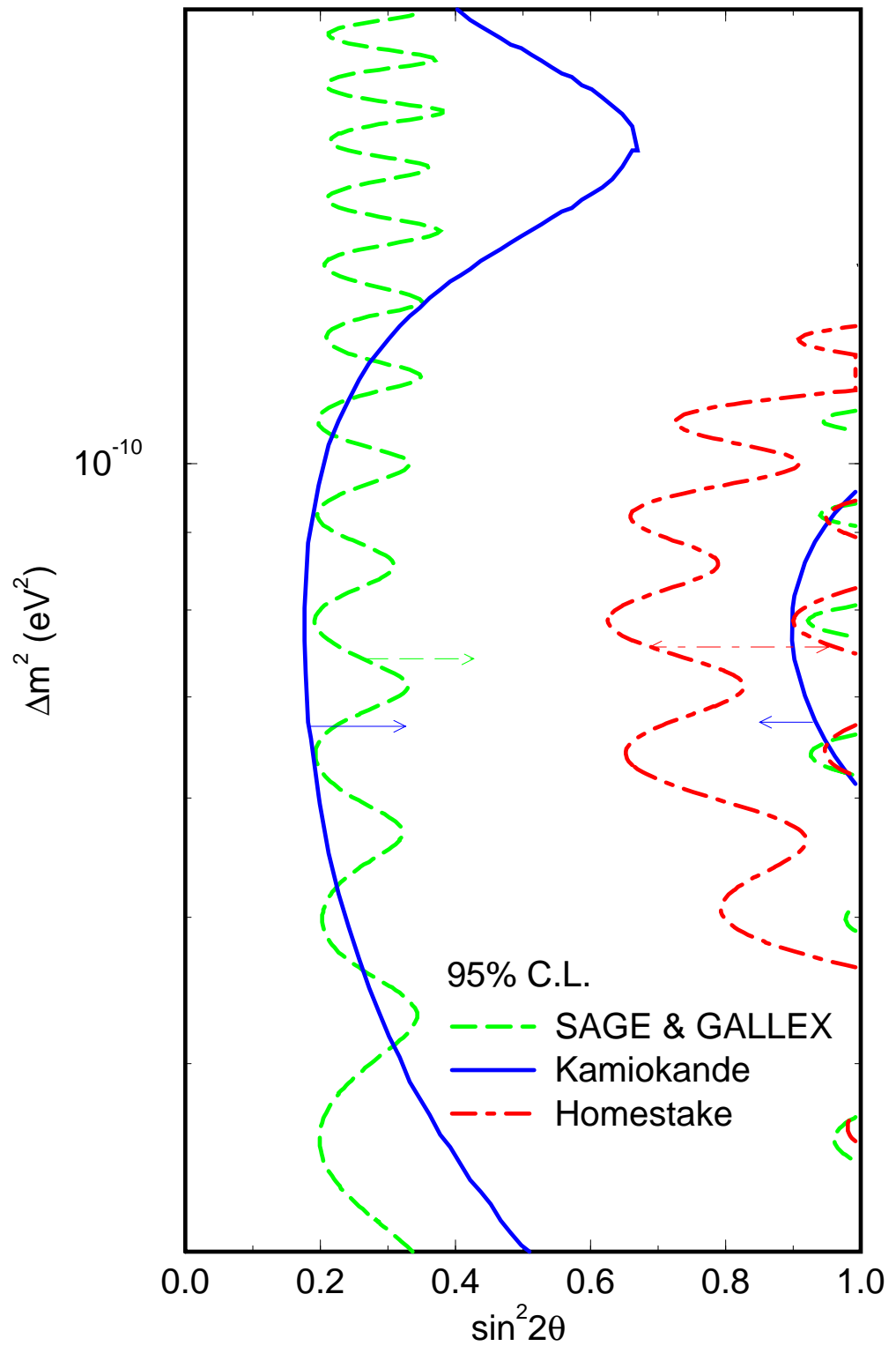
FIG. 4. The parameter space allowed by the combined observation of the Homestake, Kamiokande, and the combined gallium experiments of SAGE and GALLEX, including the theoretical uncertainties and their correlations. The Kamiokande II spectrum data are included.

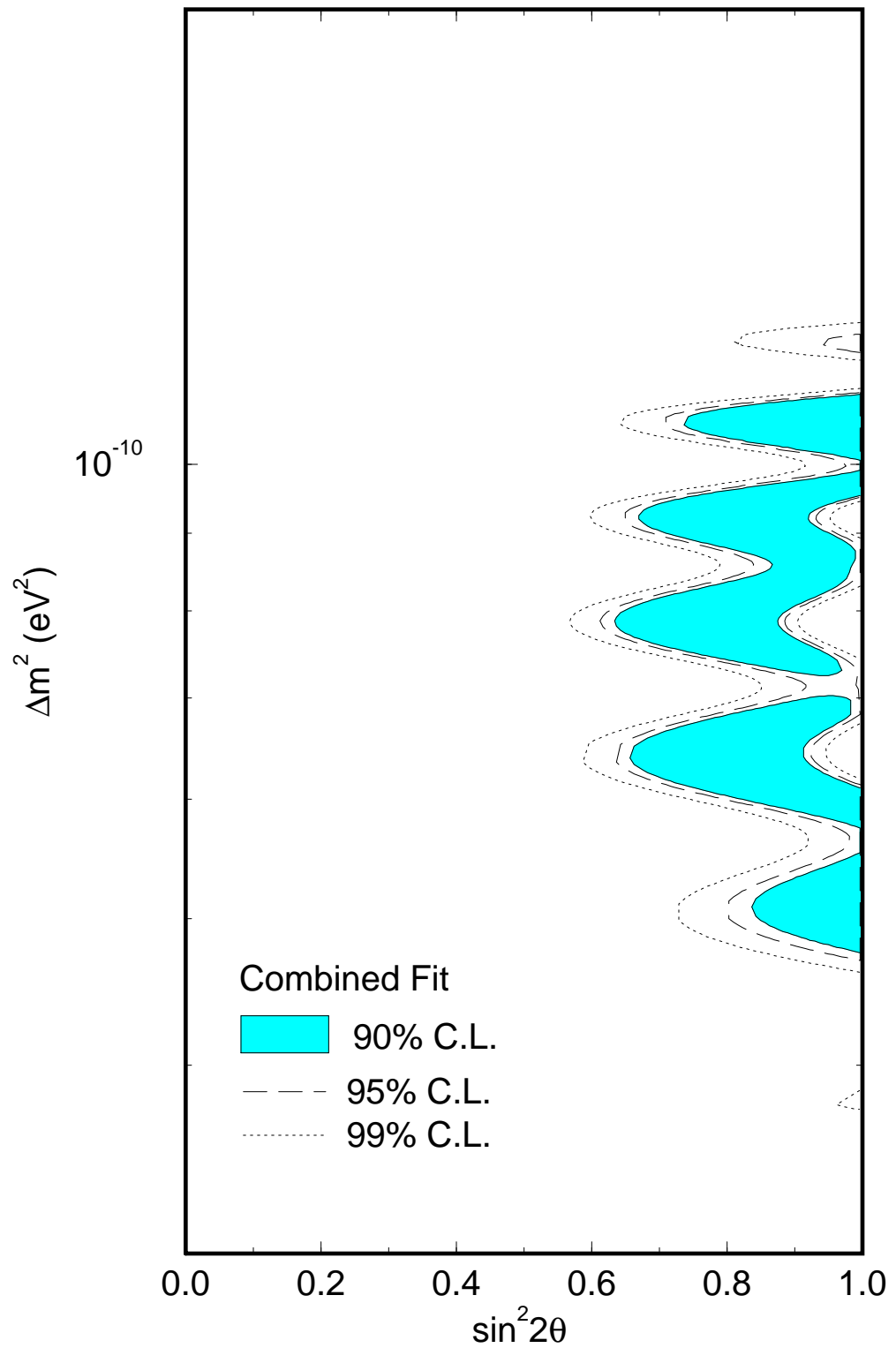
FIG. 5. The electron spectrum shape expected in SNO charged current reaction for the vacuum solutions B, D, and F (defined in Table III). Also shown are the spectra expected for the MSW solutions obtained from the combined observations. The spectrum shape of the astrophysical solutions (or no oscillations) is identical to the MSW large-angle spectrum. The spectra are normalized above the threshold (5 MeV). The error bars correspond to the statistical uncertainties for a total of 6,000 events (2 year operation).

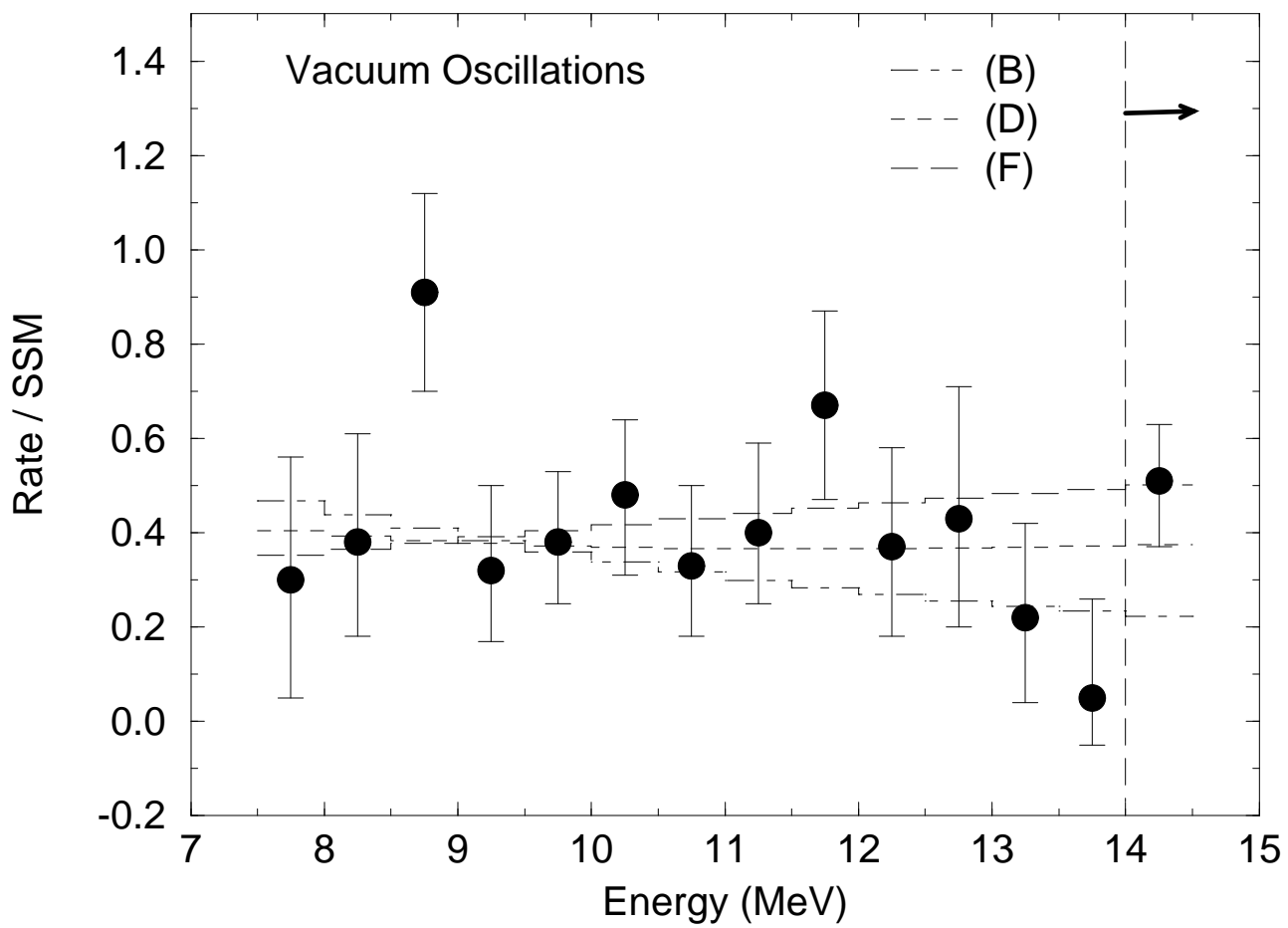
FIG. 6. The electron spectrum shape expected in Super-Kamiokande for the vacuum solutions B, D, and F (defined in Table III). Also shown are the spectra expected for the MSW solutions obtained from the combined observations. The spectrum shape of the astrophysical solutions (or no oscillations) is identical to the MSW large-angle spectrum. The spectra are normalized above the threshold (5 MeV). The error bars correspond to the statistical uncertainties for a total of 16,000 events (2 year operation).

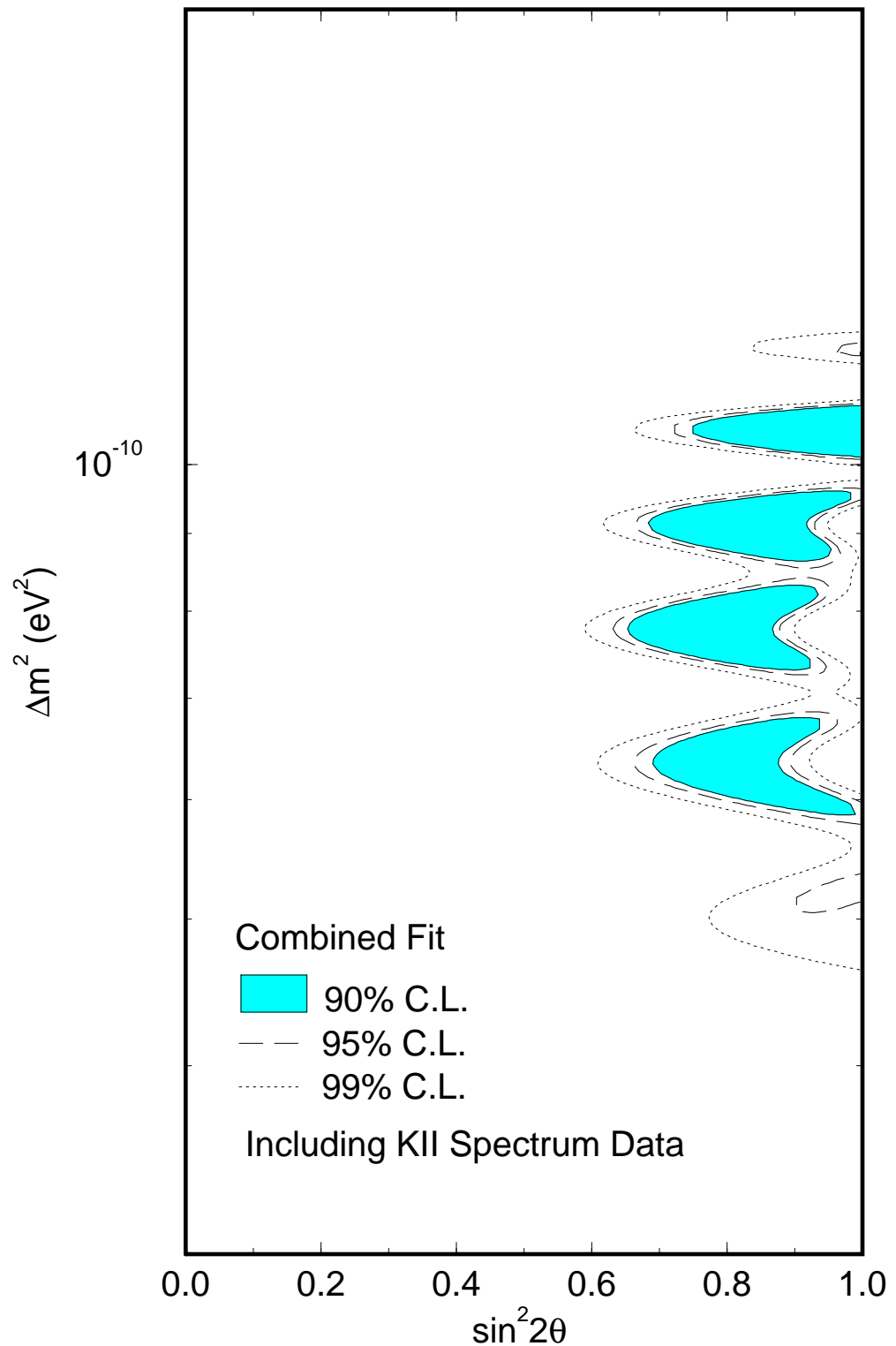
FIG. 7. The seasonal variation of the signal expected in the existing experiments for the vacuum solutions B, D, and F (see Table III). The error bars corresponds to (overly) optimistic statistical errors. The accumulated events in the existing experiments are ~ 200 , ~ 500 , and ~ 50 for Kamiokande, Homestake, and the combined gallium experiments. No significant constraint is expected from the existing experiments.

FIG. 8. The seasonal variation of the signal expected in the future experiments of SNO (charged-current reaction), Super-Kamiokande, and BOREXINO for the vacuum solutions B, D, and F (see Table III). The error bars correspond to the total events for 4 year operation. Those measurements should be sensitive enough to distinguish the vacuum oscillations from the MSW solutions and constrain the parameter space.

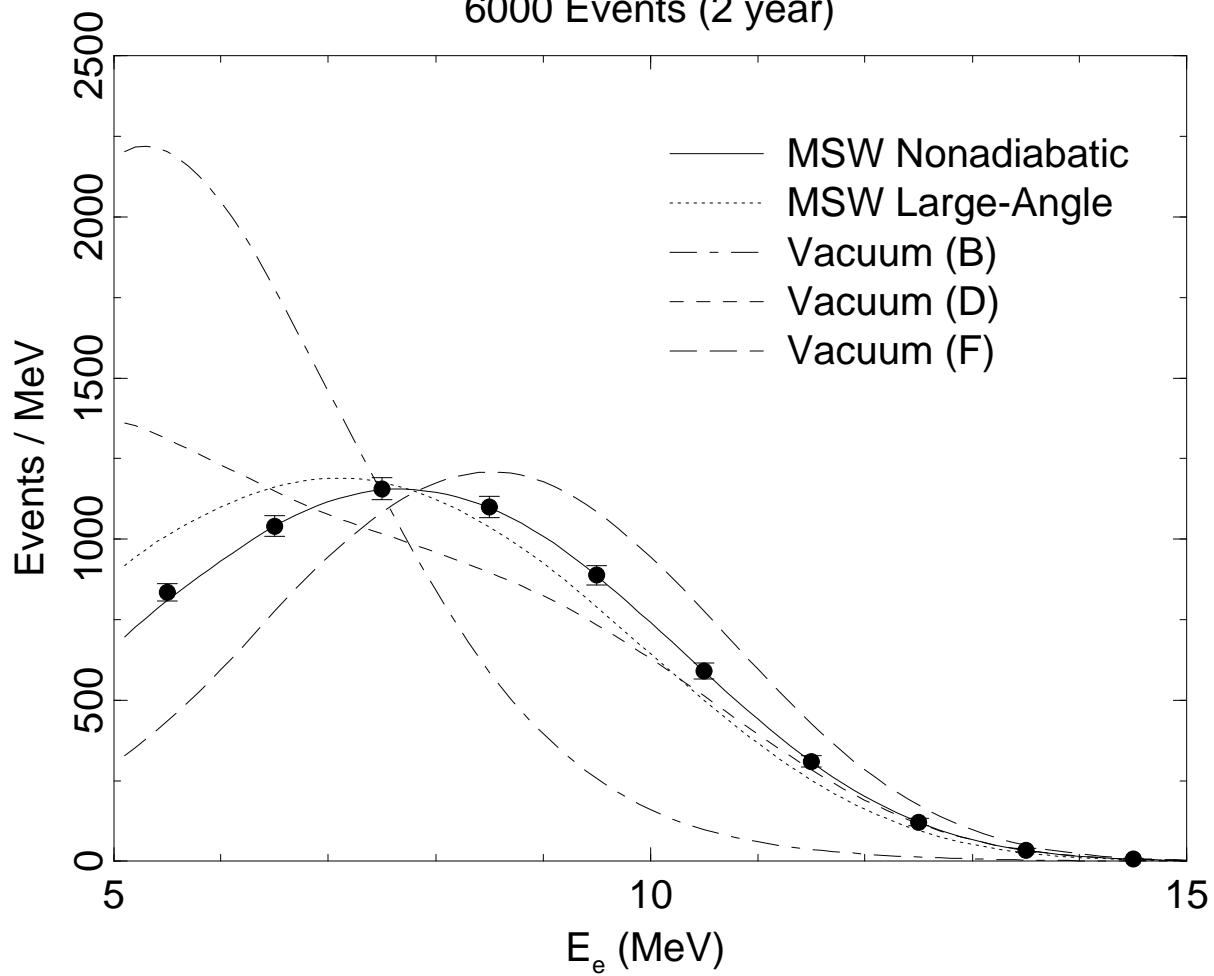








SNO CC Electron Spectrum
6000 Events (2 year)



Super-Kamiokande Electron Spectrum
16000 Events (2 year)

